Amino Acids (2010) 38:213–222
DOI 10.1007/s00726-008-0229-0

ORIGINAL ARTICLE

Antifreeze glycopeptide analogues: microwave-enhanced synthesis and functional studies

Carolin Heggemann · Carsten Budke · Benjamin Schomburg · Zsuzsa Majer · Marco Wißbrock · Thomas Koop · Norbert Sewald

Received: 14 September 2008 / Accepted: 22 December 2008 / Published online: 23 January 2009

Abstract Antifreeze glycoproteins enable life at temperatures below the freezing point of physiological solutions. They usually consist of the repetitive tripeptide unit (-Ala-Ala-Thr-) with the disaccharide α-D-galactosyl-(1–3)-*β*-*N*-acetyl-D-galactosamine attached to each hydroxyl group of threonine. Monoglycosylated analogues have been synthesized from the corresponding monoglycosylated threonine building block by microwave-assisted solid phase peptide synthesis. This method allows the preparation of analogues containing sequence variations which are not accessible by other synthetic methods. As antifreeze glycoproteins consist of numerous isoforms they are difficult to obtain in pure form from natural sources. The synthetic peptides have been structurally analyzed by CD and NMR spectroscopy in proton exchange experiments revealing a structure as flexible as reported for the native peptides. Microphysical recrystallization tests show an ice structuring influence and ice growth inhibition depending on the concentration, chain length and sequence of the peptides.

Keywords Bioorganic chemistry · Microwave synthesis · Glycopeptides · Recrystallization · Circular dichroism

C. Heggemann · B. Schomburg · M. Wißbrock · N. Sewald (✉)
Organic and Bioorganic Chemistry, Bielefeld University, Universitätsstr. 25, 33615 Bielefeld, Germany
e-mail: norbert.sewald@uni-bielefeld.de

C. Budke · T. Koop
Physical Chemistry, Bielefeld University, Universitätsstr. 25, 33615 Bielefeld, Germany

Z. Majer
Institute of Chemistry, Eötvös University, 1117 Budapest, Hungary

Abbreviations

AFGP	Antifreeze glycopeptide
AFP	Antifreeze protein
br	Broad
CD	Circular dichroism
DIPEA	*N,N*-Diisopropylethylamine
DMF	*N,N*-Dimethylformamide
EtOAc	Ethyl acetate
Fmoc	*N*-(9*H*-Fluoren-9-yl)-methoxycarbonyl
GalNAc	2-Acetamido-2-deoxy-D-galactopyranosyl-
HATU	*O*-(7-Azabenzotriazol-1-yl)-*N,N,N',N'*-tetramethyluronium hexafluorophosphate
HOAt	1-Hydroxy-7-azabenzotriazole
MeOH	Methanol
HOBt	1-Hydroxybenzotriazole
NaOMe	Sodium methoxide
NMP	1-Methyl-2-pyrrolidone
TBTU	*O*-(Benzotriazol-1-yl)-*N,N,N',N'*-tetramethyluronium tetrafluoroborate
TFA	Trifluoroacetic acid
TFE	2,2,2-Trifluoroethanol

Introduction

Glycosylated peptides and proteins have been known for a long time to play crucial roles in living organisms. Glycoproteins are involved in various biological recognition processes, e.g. cell adhesion and differentiation (Brocke and Kunz 2002; Dwek 1996; Ernst et al. 2000). In contrast to the mucin-type *O*-glycan peptides, which are present on the membrane of mammalian cells, antifreeze glycopeptides (AFGPs) are less investigated examples of biologically important glycoconjugates. They consist of the

iterative tripeptide unit (Ala-Ala-Thr)$_n$, $n = 4$–50, with minor sequence variations where alanine is partially substituted by proline and arginine. Every threonine hydroxyl group is glycosylated with the disaccharide α-D-galactosyl-(1–3)-β-*N*-acetyl-D-galactosamine (Harding et al. 2003).

Although AFGPs have been discovered in the late 1960s, their mode of action is to a large extent unknown (DeVries and Wohlschlag 1969; DeVries et al. 1970). Pure samples from natural sources are difficult to obtain and the synthesis of heavily glycosylated peptides is challenging. The activity of the glycopeptides is proven by the inhibition of ice recrystallization, thermal hysteresis, change of crystal habitus, and suppression of heterogeneous ice nucleation (Knight et al. 1984, 1988, 1995; Raymond et al. 1989; Parody-Morreale et al. 1988).

Conformational analysis by CD and NMR indicates the existence of a threefold left-handed helix similar to a polyproline type II helix, but the structure in solution is highly flexible and changes significantly upon contact with the ice surface (Bouvet and Ben 2003; Meyer and Möller 2007). The φ torsion angle of Pro is restricted to $-65° \pm 15°$ due to the pyrrolidone ring. Therefore, peptides containing Pro residues often preferentially adopt a distinct secondary structure, the polyproline II (PPII) helix ($\varphi = -75°$, $\psi = 145°$). Other amino acid residues like Gln, Asp, Lys, Gly, Ala, and Leu are also compatible with the PPII helix (Rath et al. 2005).

Synthetic and modified AFGPs have been investigated systematically by Tachibana et al. with respect to structural motifs necessary for antifreeze activity (Tachibana et al. 2004). The AFGPs examined in this context were synthesized by uncontrolled condensation of the unprotected, glycosylated tripeptide unit H-Ala-Thr(R)-Ala-OH. Different carbohydrate moieties R were introduced in this approach to identify the essential requirements for the antifreeze activity. From these results the authors concluded that the peptides adopt a polyproline II helical structure and that they require a *N*-acetyl group at the C2 position of the galactosamine together with an α-configured linkage between the carbohydrate and the threonine side chain and the γ-methyl group of the threonine to be active in antifreeze assays. The monoglycosylated α-GalNAc containing glycopeptides already showed significant activity and are easier accessible than native AFGP analogues.

Linear solid phase peptide synthesis provides, in contrast to fragment condensation, homogenous, well-defined products. Moreover, sequence variations as they occur in native AFGPs are easily accessible. A disadvantage of the stepwise method might be that the bulky glycosylated amino acids usually need long coupling times and are possibly inefficiently coupled, especially when they occur frequently in the sequence. This problem can be overcome by more active reagents and microwave assistance. Microwave irradiation, known to accelerate difficult coupling reactions, have found their way into the field of automated solid phase peptide chemistry (Matsushita et al. 2005).

In this study, we synthesized different monoglycosylated analogues of AFGPs by microwave-enhanced solid phase peptide synthesis. The conformation of the peptides was analyzed by CD and NMR and their activity was tested in microphysical recrystallization assays.

Materials and methods

General methods

All air- and moisture-sensitive reactions were carried out in a dry argon atmosphere in flame-dried glass flasks. Dichloromethane was freshly distilled from CaH_2 and toluene from Na. DMF was distilled from ninhydrine. All amino acids and the 2-chlorotrityl resin were purchased from Iris Biotech (Marktredwitz, Germany) or Orpegen (Heidelberg, Germany). Other chemicals were bought from Sigma Aldrich (Hamburg, Germany), Acros (Geel, Belgium), and VWR (Darmstadt, Germany). All chemicals were used as purchased, if not stated otherwise. Peptide synthesis was carried out with a Liberty Automated Microwave Peptide Synthesizer (CEM, Kamp-Lintfort, Germany). The maximum temperature of all cycles was set to 40°C.

Analytical reverse phase high performance liquid chromatography (RP-HPLC) was carried out on a Thermo Separation Products system consisting of a UV 6000 diode array detector and a P 4000 pump equipped with a Phenomenex HPLC guard cartridge system (C12; 4 × 3.00 mm) and a Phenomenex Jupiter 4 µ Proteo 90 Å column (C12; 250 × 4.60 mm). Flow rate 1 mL min^{-1}. Eluent A: H_2O/CH_3CN/TFA (98/1.95/0.05), Eluent B: CH_3CN/H_2O/TFA (98/1.95/0.05). Preparative RP-HPLC was carried out with a Thermo Separation Products system consisting of a UV-1000 detector and a P-4000 pump equipped with a Vydac high-performance guard column (C18) and a Phenomenex Jupiter 10 µ Proteo 90 Å column (C12; 250 × 21.20 mm) or with a Hitachi MERCK La-Chrom system consisting of a UV–Vis L-7420 detector and a L7150 pump equipped with a Vydac high-performance guard column (C18) and a Phenomenex Jupiter 10 µ 300 Å column (C18; 250 × 21.20 mm). Flow rate 7.5 mL min^{-1}. Eluent A: H_2O/CH_3CN/TFA (98/1.95/0.05), Eluent B: CH_3CN/H_2O/TFA (95/4.9/0.1). MALDI-ToF mass spectra were recorded with a Voyager DE Instrument (PE Biosystems, Weiterstadt, Germany) mounted with a 1.2 m

flight tube. Ionisation was achieved using a LSI nitrogen laser (337 nm beam, 3 ns pulse width, 3 Hz repetition rate). 2,5-Dihydroxybenzoic acid or α-cyano-4-hydroxycinnamic acid were used as the matrix. The instrument default calibration was used for calibrating the mass axis. ESI experiments were performed using a Fourier Transform Ion Cyclotron Resonance (FT-ICR) mass spectrometer APEX III (Bruker Daltonik, Bremen, Germany) equipped with a 7.0 T, 160 mm bore superconducting magnet (Bruker Analytik—Magnetics, Karlsruhe, Germany), infinity cell, and interfaced to an external (nano)ESI ion source. Nitrogen served both as the nebulizer gas and the dry gas for ESI. Optical rotations were measured on a DIP-360 digital polarimeter (Jasco, Groß-Umstadt) at 20°C. NMR spectra were obtained on a DRX 500 or an Avance 600 spectrometer (Bruker Biospin, Rheinstetten, Germany). CD analysis was carried out on a J-810 spectrometer equipped with a CDF-4265 Peltier unit for temperature control (Jasco, Groß-Umstadt). All spectra were recorded at a scanning rate of 50 nm min^{-1}, a data pitch of 0.2 nm and three accumulations. The peptide concentrations were varied between 0.05 and 0.27 mmol L^{-1} in a 0.1 or 0.02 cm quartz cell. Molar residual ellipticity $[\theta]$ was calculated according to

$$[\theta] = \theta/(10 \cdot N \cdot c \cdot l)$$

where θ is the ellipticity in millidegrees, N the number of residues, c the molar concentration in mol L^{-1} and l the cell path length in centimetre.

Synthesis of the glycosylated threonine building block

*N-(9H-Fluoren-9-yl)-methoxycarbonyl-O-(3,4,6-tri-O-acetyl-2-azido-2-deoxy-D-galactopyranosyl)-L-threonine-tert-butylester (**4**)*

Fmoc-L-threonine-*tert*-butylester (Schultz and Kunz 1993) (4.70 g, 11.8 mmol) and Ag_2CO_3 (4.60 g, 16.7 mmol) were stirred with freshly activated, powdered 4 Å molsieve (14.2 g) in dry toluene (40 mL) and dry methylene chloride (60 mL) at −5°C for 30 min. Then $AgClO_4$ (632 mg, 3.05 mmol) in dry toluene (20 mL) was added dropwise within 40 min. Subsequently, galactosyl bromide **3** (7.11 g, 18.0 mmol) in a mixture of dry toluene and methylene chloride (60 mL, 1:1) was slowly added to the solution within 15 min. The solution was stirred in the dark under argon at room temperature overnight. The suspension was diluted with methylene chloride (200 mL), filtered through Celite and washed with water (100 mL) and saturated $NaHCO_3$ solution (75 mL). After drying over Na_2SO_4, the solvent was evaporated and the residue purified by column chromatography (hexanes:EtOAc, 2:1) to give α-anomer **4** (4.84 g, 57%) and a mixture of α- and β-anomer (1.35 g, 16%). $[\alpha]_D^{20} = +75.3$ (c = 0.85, $CHCl_3$). ^{1}H NMR: (500 MHz, $CDCl_3$) $\delta = 1.38$ (d, 3H, $J = 6.4$ Hz, Hγ-Thr), 1.53 (s, 9H, CH_3-*t*Bu), 2.07 (s, 3H, CH_3CO), 2.11 (s, 3H, CH_3CO), 2.18 (s, 3H, CH_3CO), 3.67 (dd, 1H, $J = 11.5$ Hz, 3.7 Hz, H2-GalNAc), 4.10–4.15 (m, 2H, CH_2-Fmoc), 4.27–4.34 (m, 4H, Hα-Thr, CH-Fmoc, H5-GalNAc, H6a-GalNAc), 4.36–4.50 (m, 2H, Hβ-Thr, H6b-GalNAc), 5.14 (d, 1H, $J = 3.6$ Hz, H1-GalNAc), 5.37 (m, 1H, H3-GalNAc), 5.50 (d, 1H, $J = 2.5$ Hz, H4-GalNAc), 5.68 (d, 1H, $J = 9.5$ Hz, NH-Thr), 7.33–7.44, 7.65–7.67, 7.78–7.80 (m, 8H, arom.). ^{13}C NMR (125.8 MHz, $CDCl_3$) $\delta = 19.3$ (Cγ-Thr), 21.0, 21.0, 28.7 (CH_3CO), 28.3 (CH_3-*t*Bu), 47.8 (CH-Fmoc), 58.1 (C2-GalNAc), 59.6 (Cα-Thr), 62.2 (CH_2-Fmoc), 67.4 (C4-GalNAc), 67.6 (C5-GalNAc), 67.9 (C6-GalNAc), 68.4(C3-GalNAc), 76.7 (Cβ-Thr), 83.3 (C-*t*Bu), 99.6 (C1-GalNAc), 120.3, 120.3, 125.3, 125.3, 125.7, 125.7, 127.5, 128.0, 141.7, 141.7, 144.2, 144.2 (arom.), 157.4, 169.5, 169.6, 170.2, 170.8 (*C*=O). MS (ESI) 733.3 $[M + Na]^+$.

*N-(9H-Fluoren-9-yl)-methoxycarbonyl-O-(3,4,6-tri-O-acetyl-2-acetamido-2-deoxy-α-D-galactopyranosyl)-L-threonine-tert-butylester (**5**)*

Fmoc-(Ac_3GalN_3)Thr-O*t*Bu **4** (16.0 g, 22.5 mmol) was dissolved in a mixture of thioacetic acid and dry pyridine (75 mL, 2:1) and stirred for 5 h. After complete conversion the volatiles were removed on a high vacuum rotary evaporator and the residue was purified by flash chromatography on silica gel (*n*-hexanes:EtOAc, 1:1 → 0:1). Product **5** was obtained as syrup (11.6 g, 71%). $[\alpha]_D^{20} = +60.2$ (c = 0.95, $CHCl_3$). ^{1}H NMR: (500 MHz, $CDCl_3$) $\delta = 1.32$ (d, 3H, $J = 6.3$ Hz, Hγ-Thr), 1.46 (s, 9H, CH_3-*t*Bu), 1.99 (s, 3H, CH_3CO), 2.01 (s, 3H, CH_3CO), 2.04 (s, 3H, CH_3CO), 2.17 (s, 3H, CH_3CO), 4.06–4.13 (m, 3H, Hα-Thr, CH_2-Fmoc), 4.19–4.29 (m, 3H, H5-GalNAc, Hβ-Thr, CH-Fmoc), 4.43–4.51 (m, 2H, H6a-GalNAc, H6b-GalNAc), 4.60 (ddd, 1H, $J = 10.6$ Hz, 10.3 Hz, 3.1 Hz, H2-GalNAc), 4.88 (d, 1H, $J = 3.2$ Hz, H1-GalNAc), 5.09 (dd, 1H, $J = 11.3$ Hz, 2.7 Hz, H3-GalNAc), 5.39 (d, 1H, $J = 2.0$ Hz, H4-GalNAc), 5.63 (d, 1H, $J = 9.5$ Hz, NH-Thr), 6.03 (d, 1H, $J = 9.8$ Hz, NH-GalNAc),7.33–7.43, 7.64–7–67, 7.78–7.80 (m, 8H, arom.). ^{13}C NMR (125.8 MHz, $CDCl_3$) $\delta = 18.6$ (Cγ-Thr), 20.7, 20.8, 20.8, 23.2 (CH_3CO), 28.1 (CH_3-*t*Bu), 47.2, 47.3, 58.9, 62.1, 67.3, 67.4, 67.4, 68.7, 75.9 (Cβ-Thr), 83.2 (C-*t*Bu),100.0 (C1-GalNAc), 120.0, 120.1, 125.1, 125.1, 127.1. 127.1, 127.8, 127.8, 141.3, 141.3, 143.7, 143.8 (arom.), 156.5, 170.0, 170.4, 170.4, 170.5, 171.0 (*C*=O). MS (ESI) 726.9 $[M + H]^+$, 749.2 $[M + Na]^+$.

*N-(9H-Fluoren-9-yl)-methoxycarbonyl-O-(3,4,6-tri-O-acetyl-2-acetamido-2-deoxy-α-D-galactopyranosyl)-L-threonine (**6**)*

tert-Butylester **5** (918 mg, 1.26 mmol) was dissolved in a mixture of TFA and water (15 mL, 95:5) and stirred for 1.5 h. The solution was distilled azeotropically with toluene. The remaining residue was suspended in acetonitrile and water and lyophilized. Amino acid **6** (756 mg, 90%) was used in solid phase peptide synthesis without further purification. $[\alpha]_D^{20} = +67.6$ (c = 1, MeOH). ^{1}H NMR: (500 MHz, DMSO-D_6) $\delta = 1.18$ (d, 3H, $J = 6.4$ Hz, Hγ-Thr), 1.84 (s, 3H, CH_3CO), 1.92 (s, 3H, CH_3CO), 2.00 (s, 3H, CH_3CO), 2.18 (s, 3H, CH_3CO), 4.04 (d, 2H, $J = 6.1$ Hz, CH_2-Fmoc), 4.14 (dd, 1H, $J = 9.9$ Hz, $J = 1.1$ Hz, Hα-Thr), 4.17–4.25 (m, 2H, H2-GalNAc, CH-Fmoc), 4.28–4.33 (m, 2H, H5-GalNAc, Hβ-Thr), 4.42 (dd, 1H, $J = 11.2$ Hz, 7.0 Hz, H6a-GalNAc), 4.48 (dd, 1H, $J = 11.2$ Hz, 6.8 Hz, H6b-GalNAc), 4.81 (d, 1H, $J = 3.7$ Hz, H1-GalNAc), 5.04 (dd, 1H, $J = 11.7$ Hz, $J = 3.2$ Hz, H3-GalNAc), 5.31 (d, 1H, $J = 2.8$ Hz, H4-GalNAc), 7.35–7.45 (m, 4H, arom.), 7.58 (d, 1H, $J = 9.8$ Hz, NH-Thr), 7.67 (d, 1H, $J = 9.4$ Hz, NH-GalNAc), 7.73–7.76, 7.91–7.93 (m, 4H, arom.), 12.91 (s, br, 1H, COOH). ^{13}C NMR (125.8 MHz, DMSO-D_6) $\delta = 19.0$ (Cγ-Thr), 21.0, 21.0, 21.5, 23.1 (CH_3CO), 47.0 (C5-GalNAc), 47.2 (CH-Fmoc), 58.9 (Cα-Thr), 62.4 (CH_2-Fmoc), 66.0 (C6-GalNAc), 66.9 (C2-GalNAc), 67.7 (C4-GalNAc), 68.1 (C3-GalNAc), 75.4 (Cβ-Thr) 99.2 (C1-GalNAc), 120.6, 120.7, 125.6, 125.7, 127.6, 127.6, 128.1, 128.2, 141.2, 141.2, 144.2, 144.2 (arom.), 157.4, 169.9, 170.3, 170.4, 170.5, 172.2 (*C*=O). MS (ESI) 671.0 $[M + H]^+$, 693.2 $[M + Na]^+$.

Peptide synthesis

2-Chlorotrityl resin was loaded manually with Fmoc-Ala-OH. The loading was analyzed spectroscopically and quantified to be 0.6 mmol g^{-1}. The reaction vessel of the synthesizer was filled with resin (170 mg, 0.10 mmol). All steps were performed under microwave radiation at a maximum of 20 W and 40°C. Fmoc cleavage was achieved by treating the resin twice with piperidine in DMF (20%, v/v, 7 mL) for 7 min. The couplings of Fmoc-Ala-OH, Fmoc-Gly-OH, and Fmoc-Pro-OH (0.50 mmol, 5.0 eq) dissolved in DMF (2.5 mL) were accomplished in 10 min with TBTU (0.50 mmol, 5.0 eq) in DMF (1 mL) and DIPEA (1.0 mmol, 10 eq) in NMP (0.5 mL). Glycosylated threonine **6** (0.25 mmol, 2.5 eq) was preactivated for 2 min with HATU (0.28 mmol 2.8 eq) in DMF (1 mL) and transferred manually to the reaction vessel. HOAt (0.23 mmol, 2.3 eq) and DIPEA (0.55 mmol, 5.5 eq) in DMF (1 mL) were added and coupled for 15 min. Likewise, Fmoc-Thr(tBu)-OH (0.50 mmol, 5.0 eq) was used in the synthesis of the unglycosylated peptide **17**. Unreacted amino groups were capped by acetylation with acetic anhydride (5 mmol) in presence of DIPEA (1.25 mmol) and HOBt (0.1 mmol) in DMF (10 ml). After final Fmoc cleavage, the peptides were taken off from the synthesizer and the following steps were accomplished manually. The peptides were cleaved from the resin by treatment with TFA in methylene chloride (1%, v/v, 10 × 5 mL) for 5 min. *i*-Propanol was added and the volume was reduced to 5 mL by evaporation. The peptides were precipitated with cold diethylether, the crude products were dissolved in Millipore water (10 mL) and lyophilized. The acetylated peptides **10**–**12** were purified after this step for structural and microphysical analysis.

H-[Ala-Ala-Thr(Ac_3GalNAc)]$_3$-Ala-Ala-OH **11** (62 mg, 33%): $C_{78}H_{120}N_{14}O_{39}$; calc. 1877.9 (av); 1876.7837 (monoisotopic); MS (MALDI-ToF) $m/z = 1898.3$ $[M + Na]^+$, 1916.3 $[M + K]^+$.

H-[Ala-Ala-Thr(Ac_3GalNAc)]$_5$-Ala-Ala-OH **12** (45 mg, 15%): $C_{126}H_{192}N_{22}O_{63;}$ calc. 3023.0 (av); 3021.2497 (monoisotopic); MS (MALDI-ToF) $m/z = 3045.2$ $[M + Na]^+$, 3061.4 $[M + K]^+$.

For deacetylation of the carbohydrate protecting groups, the peptides were dissolved in methanol (10 mL) and the pH of the solution was adjusted to 9.5 by addition of NaOMe in methanol (1%, w/v, 15 droplets) at room temperature. After complete deprotection, the solution was neutralized with acetic acid (~5 droplets) and concentrated in vacuo. The peptides were purified by preparative RP-HPLC and identified by MALDI-ToF-MS analysis.

H-[Ala-Ala-Thr(GalNAc)]$_3$-OH **7** (23 mg, 15%): $C_{60}H_{102}N_{14}O_{30}$; calc. 1499.5 (av); 1498.6886 (monoisotopic); MS (MALDI-ToF) $m/z = 1522.0$ $[M + Na]^+$, 1538.5 $[M + K]^+$; HRMS (ESI): 772.33294 $[M + 2Na]^{2+}$.

H-[Ala-Ala-Thr(GalNAc)]$_4$-Ala-Ala-OH **8** (25 mg, 13%): $C_{78}H_{132}N_{18}O_{39}$; calc. 1946.0 (av); 1944.8899 (monoisotopic); MS (MALDI-ToF) $m/z = 1967.2$ $[M + Na]^+$, 1984.5 $[M + K]^+$; HRMS (ESI): 995.45432 $[M + 2Na]^{2+}$, 1006.42422 $[M\text{-}H + 3Na]^{2+}$.

H-[Ala-Ala-Thr(GalNAc)]$_5$-Ala-Ala-OH **9** (28 mg, 12%): $C_{96}H_{162}N_{22}O_{48}$; calc. 2392.4 (av); 2391.0912 (monoisotopic); MS (MALDI-ToF) $m/z = 2414.7$ $[M + Na]^+$, 2431.1 $[M + K]^+$; HRMS (ESI): 820.02081 $[M + 3Na]^{3+}$.

Ac-[Ala-Ala-Thr(GalNAc)]$_3$-Ala-Ala-OH **10** (5 mg, 31%): $C_{62}H_{104}N_{14}O_{31}$; calc. 1541.6 (av); 1540.6992 (monoisotopic); MS (MALDI-ToF) $m/z = 1563.9$ $[M + Na]^+$, 1579.5 $[M + K]^+$; HRMS (ESI): 793.33863 $[M + 2Na]^{2+}$.

H-Ala-Ala-Thr(GalNAc)-Pro-Ala-Thr(GalNAc)-Ala-Ala-Thr(GalNAc)-Pro-Ala-OH **13** (17 mg, 11%): $C_{64}H_{106}N_{14}O_{30}$; calc. 1550.7 (av); 1551.6022 (monoisotopic); MS (MALDI-

ToF) $m/z = 1573.7$ $[M + Na]^+$, 1590.0 $[M + K]^+$; HRMS (ESI): 787.35696 $[M + Na + H]^{2+}$, 798.34940 $[M + 2Na]^{2+}$.

H-Ala-Ala-Thr(GalNAc)-Gly-Ala-Thr(GalNAc)-Ala-Ala-Thr(GalNAc)-Pro-Ala-OH **14** (18 mg, 12%): $C_{61}H_{102}N_{14}O_{30}$; calc. 1511.5 (av); 1510.6886 (monoisotopic); MS (MALDI-ToF) $m/z = 1533.0$ $[M + Na]^+$, 1549.2 $[M + K]^+$; HRMS (ESI): 756.35269 $[M + 2H]^{2+}$, 767.34306 $[M + H+Na]^{2+}$, 778.33396 $[M + 2Na]^{2+}$.

H-Ala-Ala-Thr(GalNAc)-Ser-Ala-Thr(GalNAc)-Ala-Ala-Thr(GalNAc)-Pro-Ala-Thr(GalNAc)-Ala-Ala-OH **15** (8 mg, 5%): $C_{62}H_{104}N_{14}O_{31}$; calc. 1541.6 (av); 1540.6992 (monoisotopic); MS (MALDI-ToF) $m/z = 1564.6$ $[M + Na]^+$, 1580.9 $[M + K]^+$; HRMS (ESI): 771.35859 $[M + 2H]^{2+}$, 782.34779 $[M + H+Na]^{2+}$, 793.33863 $[M + 2Na]^{2+}$.

H-[Pro-Ala-Thr(GalNAc)]$_4$-Pro-Ala-OH **16** (7 mg, 5%): $C_{88}H_{142}N_{18}O_{39}$; calc. 2076.2 (av), 2074.9682 (monoisotopic); MS (MALDI-ToF) $m/z = 2096.4$ $[M + Na]^+$, 2112.8 $[M + K]^+$; HRMS (ESI): 1038.49018 $[M + 2H]^{2+}$, 1049.48155 $[M + H+Na]^{2+}$, 1060.47287 $[M + 2Na]^{2+}$.

H-[Ala-Ala-Thr]$_4$-Ala-Ala-OH **17** (19 mg, 16%): $C_{46}H_{80}N_{14}O_{19}$; calc. 1133.2 (av); 1132.5724 (monoisotopic); MS (MALDI-ToF) $m/z = 1154.8$ $[M + Na]^+$, 1171.1 $[M + K]^+$.

Microphysical recrystallization analysis

The antifreeze activity experiments were performed employing an optical microscope (Olympus BX51) in bright field transmission mode. In the experiments the temperature was adjusted by placing the samples on a temperature-controlled silver block inside a cold stage (Linkam MDBCS 196). Both the interior and the upper window of the cold stage were purged with dry nitrogen to avoid condensation of ambient water vapour. The experimental procedures have been described previously (Budke and Koop 2006) and were used here with minor modifications. Briefly, purified peptides were dissolved at varying concentrations (depending on the activity of the peptide) between 2 and 1,400 μg mL^{-1} in aqueous 45 wt% sucrose stock solutions. For each experiment, about 2 μL of such a solution were placed between two circular 14 mm glass cover slips, which were pressed together producing a sample film with a final thickness of about 10–20 μm. A sample was positioned onto the cold stage and cooled to −50°C at a rate of −20°C min^{-1}. It was then reheated to −8°C at 10°C min^{-1}, where the polycrystalline ice was annealed for 120 min. During this time pictures were taken every minute using a digital video camera.

Results and discussion

The easily obtainable (−)-tri-*O*-acetyl-D-galactal **1** was used as starting material for the building block synthesis (Mitchell et al. 2001). It was converted into the 2-azido sugar **2** by azidonitration (Lemieux and Ratcliffe 1979). The glycosylation reaction succeeded using silver carbonate and silver perchlorate as promotors and the bromide **3** as glycosyl donor (Paulsen and Adermann 1989). Subsequent transformation to the acetamide and deprotection gave the Fmoc-protected building block **6** in good yields. Azidonitration and glycosylation represent the key steps of the reaction sequence (Scheme 1).

The glycosylated threonine building block was used in microwave-enhanced, semi-automated peptide synthesis. Peptides containing different numbers of repeating units (**7–9**) and different degrees of acetylation (**10–12**) were prepared using this method. In addition, an analogue containing two proline residues (**13**) designed to promote polyproline II helix formation, a more flexible analogue containing glycine (**14**), a peptide containing the more polar serine (**15**) and one with the repeating sequence -Pro-Ala-Thr(GalNAc)- (**16**) have been synthesized. For comparison the aglycon backbone of the 14-mer (**17**) was prepared as well (Scheme 2).

The peptides were synthesized semi-automatically using a microwave synthesizer with the maximum temperature set to 40°C. The microwave-enhanced synthesis reduced

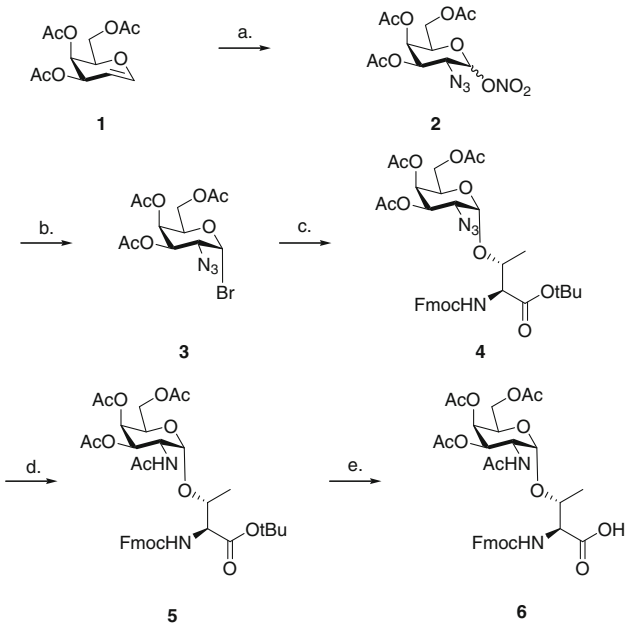

Scheme 1 **a** CAN, NaN_3, CH_3CN, 35%; **b** LiBr, CH_3CN, 97%; **c** Fmoc-Thr-OtBu, Ag_2CO_3, $AgClO_4$, toluene/CH_2Cl_2, 73%, $\alpha:\beta = 3:1$; **d** AcSH, pyridine, 71%; **e** TFA/H_2O (95/5), 90%

the time for one coupling cycle from 3 h to 45 min. The crude products were already quite pure and contained only small amounts of truncated sequences. Usually only a single purification step after deacetylation was necessary. The SPPS yielded between 4 and 33% of the peptides. Epimerization was not detected in the synthesis. Increasing the temperatures and shortening the microwave irradiation times during the cycles did not further accelerate the reaction. Instead it led to massive decomposition and deglycosylation of the peptides.

For peptides **7–12** and **16** only one peak was observed in the analytical HPLC. In contrast to this, the other proline containing peptides **13–15** gave different conformers depending on their proline content which were separable by HPLC. Compound **13** was an equilibrium mixture of three different conformers. The conformers could be enriched by preparative HPLC, but equilibrated quickly after separation. Compounds **14** and **15** contained one major conformer and a second minor conformer.

The CD spectra of the AFGP analogues **7–9** (Fig. 1) show a maximum at 216 nm and a minimum at ≈195 nm. The curves indicate the existence of a threefold left-handed helical structure as it has been proposed for native AFGP (Bush et al. 1981). Typical CD spectra of a PPII helix in water are characterized by a negative band at ≈200 nm and a weaker positive band at ≈217–225 nm (Makowska et al. 2006). Increasing Pro contents has been associated with a red-shift of the negative band to ≈205 nm because of the tertiary amide chromophore. However, CD signatures with negative bands just below 200 nm and positive bands at ≈218 nm are usually associated with random coil structures (Rath et al. 2005). It is still under debate whether proteins assumed to be present in a random coil structure might be more accurately described as comprising largely PPII helices (Makowska et al. 2006).

The CD traces displayed in Fig. 1 show that the secondary structure does not change significantly for the longer peptides **8** and **9**, which would hint at distinct stabilization of the secondary structure in the 14-peptide **8**, which does not increase upon chain elongation.

Direct comparison of the 11-peptide **7** with its [Pro^4,-Pro^{10}]-containing correlate **13**, the [Gly^4,Pro^{10}]-derivative **14**, the [Ser^4,Pro^{10}]-analogue **15**, and the 14-peptide **16**, that contains five Pro residues shows that replacement of Gly^4 by Ser does not alter the secondary structure significantly. Surprisingly, the introduction of proline in peptides **13**, **14** and **15** does not increase the CD effect (Fig. 2). The maximum at ∼215 nm distinctly decreases and the minimum at 195 nm is less pronounced. Presumably, proline residues stabilize local, non-periodical secondary structure motifs (turns) at the expense of helical structure in the smaller peptides.

As expected, an increasing Pro contents results in a red-shifted negative band between 200 and 206 nm because of the contribution of the tertiary amide chromophores. The CD curve of peptide **16** does not show a maximum and the minimum is shifted to 204 nm (Fig. 2).

The unglycosylated peptide backbone **17** has a completely different CD signature with a maximum at 198 nm and a minimum at 218 nm, which is typical for a β-strand or β-turn motif. Although the CD spectra of the β-strand and the PP II helix conformations differ dramatically, the two conformations are very close in φ/ψ space (Bhatnagar and Gough 1996). This structural change seems to be influenced by the sugar moieties which do not display any CD effect in the measuring range.

In addition, the CD effect is not significantly influenced by acetylation of either the *N*-terminus or the carbohydrates as revealed by a comparison of the CD curves of **7**, **10**, and **11** as well as **9** and **12** (not shown).

Measurements of compounds **8**, **9** and **12** in the helix stabilizing solvent TFE revealed that the extrema diminished distinctly (not shown). The CD effect of compound **16** in TFE was not influenced as significantly as for the other proline derivatives. The effect was only slightly reduced and the minimum was blue-shifted. It is generally accepted that aqueous solvation stabilizes PPII formation (Horng and Raines 2006). Solvation of the carbohydrate hydroxyl groups in aqueous solution might be another possible reason. Without any aqueous solvation, only intramolecular hydrogen bonds can be formed and the structure might collapse. This is equally true for the acetylated compound **12** whose carbohydrate moieties are hydrogen bond acceptors, but not donors.

Temperature-dependent CD spectra were recorded in order to clarify the prevalence of either the PPII conformation or of a random coil (Fig. 3). An isodichroic point with intersecting CD curves recorded under different conditions was observed at ≈205 nm. The dependence of the CD spectra on the temperature is hence being interpreted as a shift in the conformational equilibrium between a polyproline II helix and the random coil (Makowska et al. 2006).

Proton–deuterium exchange experiments of the 14-mer peptides **7**, **13**, **14**, and **15** in H_2O/D_2O revealed almost complete exchange of the amide protons within a few minutes. Only the protons of the carbohydrate amide moiety and the threonine amide protons were exchanged more slowly. This hints at a more shielded hydrogen bond at this position.

The CD and the NMR experiments indicate a highly flexible structure of the peptides in solution. Therefore, we suggest that most antifreeze glycopeptides under investigation are present as a polyproline II helix with different degree of flexibility.

Scheme 2 Different monoglycosylated AFGP analogues including sequence variations

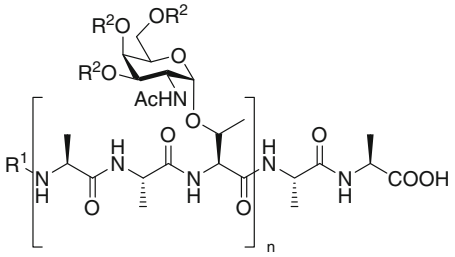

	n = 3	n = 4	n = 5
R^1=H, R^2=H	7	8	9
R^1=Ac, R^2=H	10	-	-
R^1=H, R^2=Ac	11	-	12

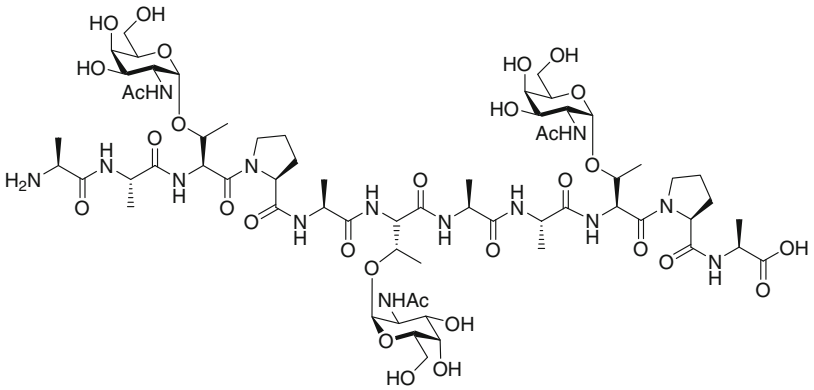

13

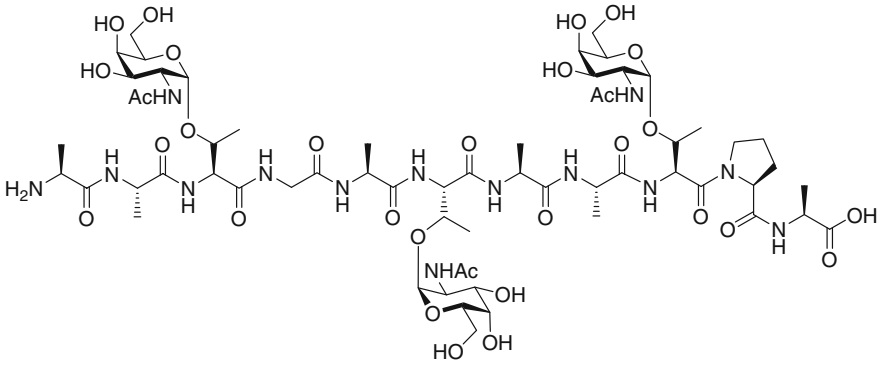

14

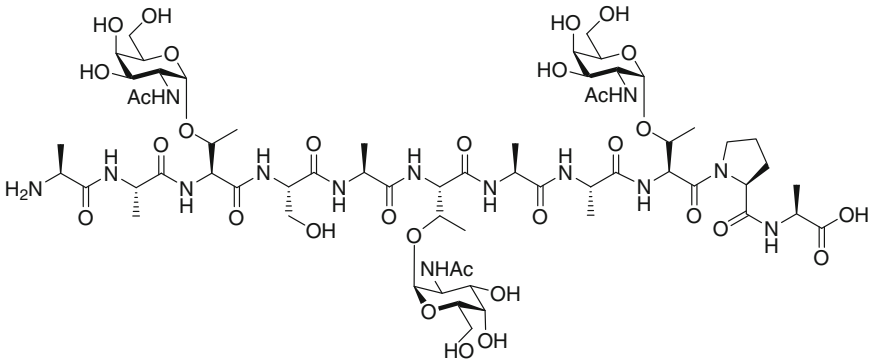

15

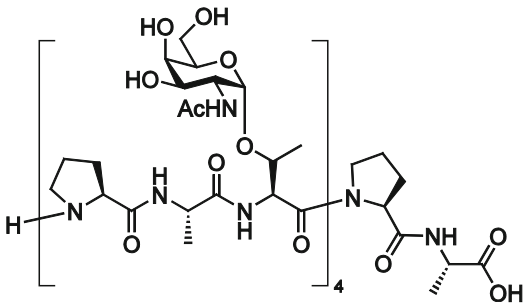

16

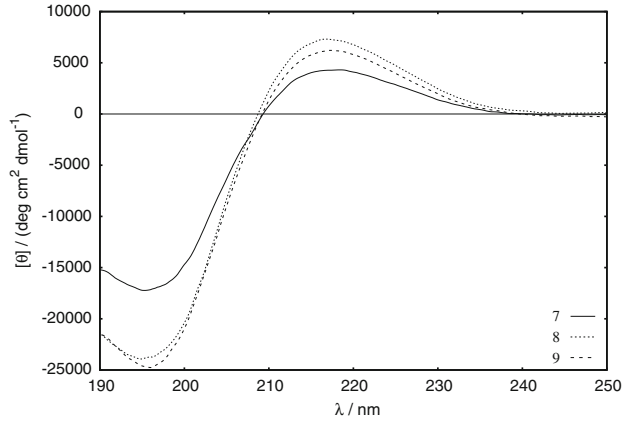

Fig. 1 CD specta of synthetic AFGP analogues containing different repeating units (water, 10°C, 0.2 mg mL^{-1})

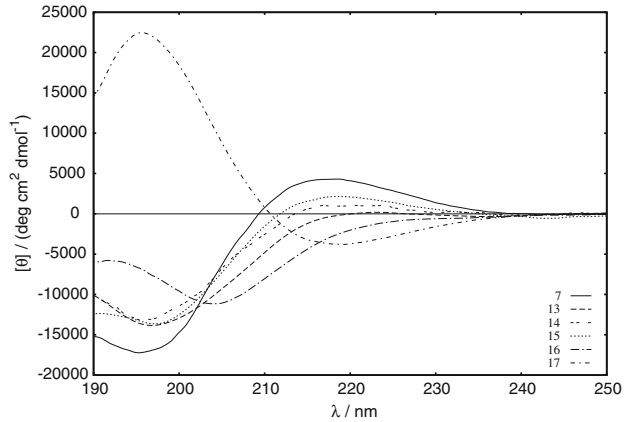

Fig. 2 CD spectra of different 11-mer or 14-mer AFGP analogues and the 14-mer aglycon backbone **17** (water, **7**, 10°C, 0.2 mg mL^{-1}; **13**, **14**, **16**, **17**, 10°C, 0.4 mg mL^{-1}; **15**, 12°C, 0.4 mg mL^{-1})

One method for the determination of antifreeze activity of antifreeze proteins and antifreeze glycoproteins is the ice recrystallization inhibition technique (Knight et al. 1988; Knight et al. 1995). Ice recrystallization occurs in polycrystalline ice samples and describes a process where larger ice crystals grow at the expense of smaller ones in an Ostwald ripening process. The kinetics of this process is commonly determined by the diffusion of water molecules from the smaller to the larger crystals through the liquid phase between adjacent ice crystals. However, in the presence of specific inhibitors such as AFPs and AFGPs the Ostwald ripening process is reduced by adsorption of the effectors to certain ice crystal faces. These faces grow at a much slower rate and lead to a particular ice crystal habitus that is very specific for AFPs and AFGPs (Bush et al. 1981; Yeh and Feeney 1996; Davies et al. 2002).

The influence of synthetic peptide **8** on ice recrystallization is shown in Fig. 4. Ice crystals in control solutions without peptides are circular in shape (Fig. 4a), as the

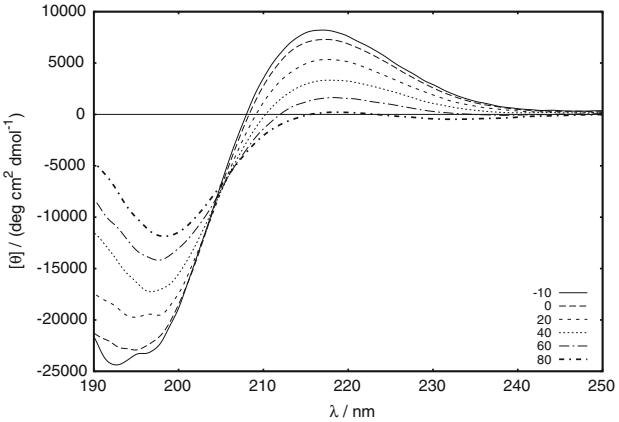

Fig. 3 Temperature dependent CD spectra of AFGP analogue **9** in water

ice/liquid interface energy is minimized in this geometry. In contrast, ice crystals in the presence of **8** revealed a hexagonal crystal habitus (Fig. 4b), indicating the specific interaction between ice and the glycopeptides. Similar results were obtained for peptides **7** and **9**.

The overall effect of the adsorption process of peptides **7–9** on the kinetics of ice recrystallization is shown in Fig. 5. All three glycopeptides clearly revealed antifreeze activity as they strongly inhibit ice recrystallization. However, the maximum inhibition was achieved at a concentration that is specific for each particular glycopeptide. The smallest peptide **7** revealed maximum inhibition only at concentrations larger than about ~1,200 μg mL^{-1} (0.8 mM) (Fig. 5b). At lower concentrations, the inhibition was similar to that of the control solution (Fig. 5a); at higher concentrations no further changes were observed. In comparison to the results at 1,200 μg mL^{-1} (0.8 mM) of **7** shown in Fig. 5b, **8** revealed a similar activity at ~200 μg mL^{-1} (0.1 mM) (Fig. 5c), and **9** already at ~30 μg mL^{-1} (12.5 μM) (Fig. 5d). The proline containing glycopeptides **13–15** were only slightly active at a concentration of 4,000 μg mL^{-1}. While compounds **14** with a Gly and Pro residue and **15** with a Ser and Pro residue both

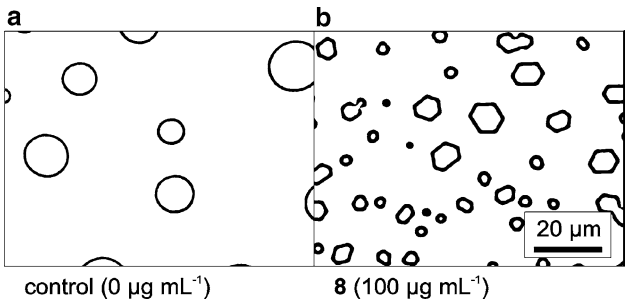

Fig. 4 Optical microphotographs of ice crystals formed in aqueous 45 wt% sucrose solutions after annealing at −8°C for 120 min: **a** control solution without peptides, **b** 8, (100 μg mL^{-1}). Both pictures were contrast-enhanced for better visibility

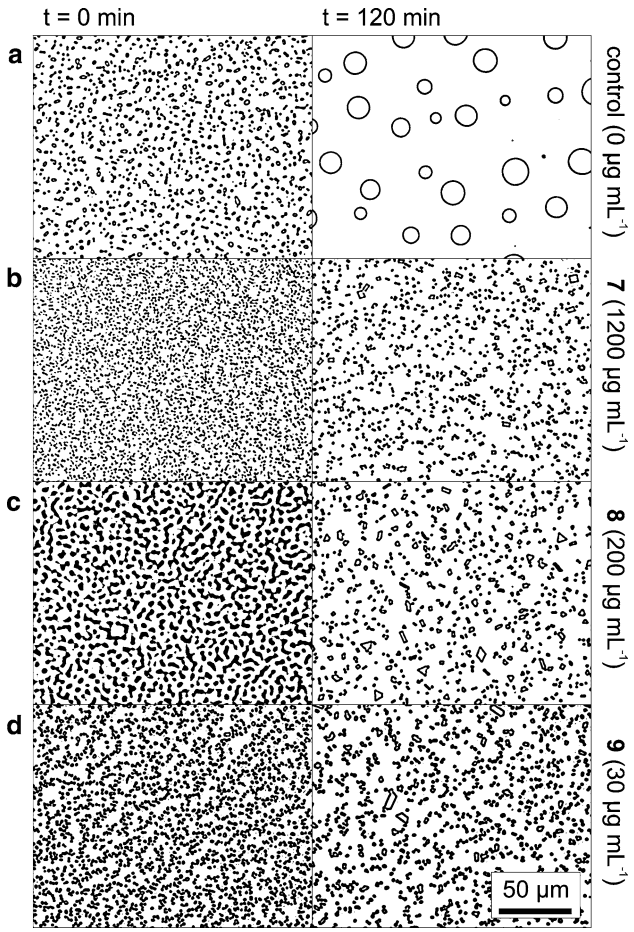

Fig. 5 Optical microphotographs of ice crystals formed in aqueous 45 wt% sucrose solutions after annealing at −8°C for 0 and 120 min: **a** control solution without peptides, **b 7** (1,200 µg mL^{-1}), **c 8** (200 µg mL^{-1}), **d 9** (30 µg mL^{-1}). All pictures were contrast-enhanced for better visibility

exhibited hexagonal ice crystals but only small inhibition activity, peptide **13** did not show any influence on the crystals up to a concentration of 4,000 µg mL^{-1}. Probably, two proline substitutions prevent the peptide **13** from adopting the periodic, active conformation, e.g. by non-periodic turn formation around the proline residues. This effect is partially suspended by glycine in compound **14** as it provides more flexibility in the peptide backbone and by serine in **15** which is as sterically demanding as alanine but is a hydrogen bond donor. One more hydrogen bond could support forming an interaction between the peptide and the ice surface. Both peptides **14** and **15** showed at least a reduced activity at the investigated concentrations. The tetraglycosylated 14-peptide **16** was only slightly less active than compound **8**. These results show that the existence of a periodical sequence motif stabilizing a PPII helical structure is crucial for antifreeze activity and non-periodically introduced proline residues abolish antifreeze activity in shorter native AFGPs. Moreover, the results show that the extent of the inhibition effect depends on both the concentration and the molar mass of the inhibitor. A similar behaviour was observed with natural antifreeze proteins and glycoproteins (Yeh and Feeney 1996) and also with synthetic polymers (Budke and Koop 2006). While the concentration dependence can be explained by a larger surface coverage of ice with the peptides at higher concentrations, the molar mass dependence is most likely due to a stronger adsorption to the ice mediated by multiple hydrogen bonds. This is in agreement with theoretical adsorption models for antifreeze proteins (Li et al. 2006). This supposition is also supported by the fact that the *N*- and *O*-acetylated peptides **10** (no activity at 1,000 µg mL^{-1}) and **12** (activity at 1,000 µg mL^{-1}) showed a distinctly reduced activity.

In conclusion, microwave-enhanced solid phase peptide synthesis is an excellent tool for the preparation of heavily glycosylated peptides regarding the improvement of purity, synthesis time, and yield. In addition, our experimental results clearly indicate that peptides **7–9** synthesized by this approach exhibit significant antifreeze activity and ice structuring activity, even though they contain only monosaccharide moieties. The proline containing peptides **13**, **14** and **15** are less active or inactive. The irregular incorporation of proline does not lead to a highly active conformation because of non-periodic turn formation, while the peptide **16** with the repeating sequence -Pro-Ala-Thr(GalNAc)- adopts a regular periodic secondary structure and hence is active in antifreeze assays.

Acknowledgments The authors gratefully acknowledge support from DFG (SFB 613).

References

Bhatnagar RS, Gough CA (1996) Circular dichroism of collagen and related polypeptides. In: Fasman GD (ed) Circular dichroism and the conformational analysis of biomolecules. New York, Plenum Press, p 198

Bouvet V, Ben RN (2003) Antifreeze glycoproteins—structure, conformation, and biological applications. Cell Biochem Biophys 39:133–134

Brocke C, Kunz H (2002) Synthesis of tumor-associated glycopeptide antigens. Biorg Med Chem 10:3085–3112

Budke C, Koop T (2006) Ice recrystallization inhibition and molecular recognition of ice faces by poly(vinyl alcohol). Chemphyschem 7:2601–2606

Bush CA, Feeney DT, Osuga T, Ralapati S, Yeh Y (1981) Antifreeze glycoprotein. Conformational model based on vacuum ultraviolet circular dichroism data. Int J Peptide Protein Res 17:125–129

Davies PL, Baardsnes J, Kuiper MJ, Walker VK (2002) Structure and function of antifreeze proteins. Philos Trans R Soc London Ser B 357:927–933

DeVries AL, Wohlschlag DE (1969) Freezing resistance in some Antarctic fishes. Science 163:1073–1075

DeVries AL, Komatsu SK, Feeney RE (1970) Chemical and physical properties of freezing point depressing glycoproteins from Antarctic fishes. J Biol Chem 245:2901–2908

Dwek RA (1996) Glycobiology: toward understanding the function of sugars. Chem Rev 96:683–720

Ernst B, Hart GW, Sinaÿ P (2000) Carbohydrates in chemistry and biology. Wiley-VCH, Weinheim

Harding MM, Anderberg PI, Haymet AD (2003) 'Antifreeze' glycoproteins from polar fish. Eur J Biochem 270:1381–1392

Horng JC, Raines RT (2006) Stereoelectronic effects on polyproline conformation. Protein Sci 15:74–83

Knight CA, DeVries AL, Oolman LD (1984) Fish antifreeze protein and the freezing and recrystallization of ice. Nature 308:295–296

Knight CA, Hallet J, DeVries AL (1988) Solute effects in ice recrystallization: an assessment technique. Cryobiology 25:55–60

Knight CA, Wen D, Laursen RA (1995) Nonequilibrium antifreeze peptides and the recrystallization of ice. Cryobiology 32:23–34

Lemieux RU, Ratcliffe RM (1979) The azidonitration of tri-*O*-acetyl-D-galactal. Can J Chem 57:1244–1251

Li QZ, Yeh Y, Liu JJ, Feeney RE, Krishnan VV (2006) A two-dimensional adsorption kinetic model for thermal hysteresis activity in antifreeze proteins. J Chem Phys 124:204702

Makowska J, Rodziewicz-Motowidło S, Bagińska K, Vila JA, Liwo A, Chmurzyński L, Scheraga HA (2006) Polyproline II conformation is one of many local conformational states and is not an overall conformation of unfolded peptides and proteins. Proc Natl Acad Sci USA 103:1744–1749

Matsushita T, Hinou H, Kurogochi M, Shimizu H, Nishimura SI (2005) Rapid microwave-assisted solid-phase glycopeptide synthesis. Org Lett 7:877–880

Meyer B, Möller H (2007) Conformation of glycopeptides and glycoproteins. Top Curr Chem 267:187–251

Mitchell SA, Pratt MR, Hruby VJ, Polt R (2001) Solid-phase synthesis of *O*-linked glycopeptide analogues of enkephalin. J Org Chem 66:2327–2342

Parody-Morreale A, Murphy KP, Dicera E, Fall R, DeVries AL, Gill SJ (1988) Inhibition of bacterial ice nucleators by fish antifreeze glycoproteins. Nature 333:782–783

Paulsen H, Adermann K (1989) Synthese von *O*-glycopeptid-sequenzen des *N*-terminus von interleukin 2. Liebigs Ann Chem 109:751–769

Rath A, Davidson AR, Deber CM (2005) The structure of "unstructured" regions in peptides and proteins: role of the polyproline II helix in protein folding an recognition. Biopolymers (Pept Sci) 80:179–185

Raymond JA, Wilson P, DeVries AL (1989) Inhibition of growth of nonbasal planes in ice by fish antifreezes. Proc Natl Acad Sci USA 86:881–885

Schultz M, Kunz H (1993) Synthetic *O*-glycopeptides as model substrates for glycosyltransferases. Tetrahedron Ass 4:1205–1220

Tachibana Y, Fletcher GL, Fujitani N, Tsuda S, Monde K, Nishimura SI (2004) Antifreeze glycoproteins: elucidation of the structural motifs that are essential for antifreeze activity. Angew Chem 43:856–862

Yeh Y, Feeney RE (1996) Antifreeze proteins: structures and mechanisms of function. Chem Rev 96:601–617